Publisher Version: https://doi.org/10.1039/C6DT01467D

Anticancer potential of a photoactivated transplatin derivative containing the methylazaindole ligand mediated by ROS generation and DNA cleavage

Jitka Pracharova,[a] Tereza Radosova Muchova,[b] Eva Dvorak Tomastikova,[c] Francesco P. Intini,[d] Concetta Pacifico,[d] Giovanni Natile,[d] Jana Kasparkovab,[e] and Viktor Brabec[e]*

[a]Department of Biophysics, Centre of the Region Haná for Biotechnological and Agricultural Research, Palacký University, Šlechtitelů 11, 783 41 Olomouc, Czech Republic
[b]Department of Biophysics, Faculty of Science, Palacký University, Šlechtitelů 27, CZ-78371 Olomouc, Czech Republic
[c]Institute of Experimental Botany, Centre of the Region Haná for Biotechnological and Agricultural Research, Šlechtitelů 31, 78371 Olomouc, Czech Republic
[d]Department of Chemistry, University of Bari "Aldo Moro", 70125 Bari, Italy
[e]Institute of Biophysics, Academy of Sciences of the Czech Republic, v.v.i., Královopolská 135, CZ-61265 Brno, Czech Republic. E-mail: brabec@ibp.cz

The limitations associated with the clinical utility of conventional platinum anticancer drugs have stimulated research leading to the design of new metallodrugs with improved pharmacological properties, particularly with increased selectivity for cancer cells. Very recent research has demonstrated that photoactivation or photopotentiation of platinum drugs can be one of the promising approaches to tackle this challenge. This is so because the application of irradiation can be targeted exclusively to the tumor tissue so that the resulting effects could be much more selective and targeted to the tumor. We show in this work that the presence of 1-methyl-7-azaindole in *trans*-[$PtCl_2(NH_3)(L)$] (L = 1-methyl7-azaindole, compound **1**) markedly potentiated the DNA binding ability of **1** when irradiated by UVA light in a cell-free medium. Concomitantly, the formation of cytotoxic bifunctional cross-links was markedly enhanced. In addition, **1**, when irradiated with UVA, was able to effectively cleave the DNA backbone also in living cells. The incorporation of 1-methyl-7-azaindole moiety had also a profound effect on the photophysical properties of **1**, which can generate singlet oxygen responsible for the DNA cleavage reaction. Finally, we found that **1**, upon irradiation with UVA light, exhibited a pronounced dose-dependent decrease in viability of A2780 cells whereas it was markedly less cytotoxic if the cells were treated in the absence of light. Hence, it is possible to conclude that **1** is amenable to photodynamic therapy.

Introduction

Bifunctional platinum complexes such as cisplatin [*cis*-diamminedichloridoplatinum(II)], carboplatin [*cis*-diammine(1,1cyclobutanedicarboxylato)platinum(II)] and oxaliplatin [*R,R*-cyclohexane-1,2-diamineoxalatoplatinum(II)] are widely used as effective drugs in cancer chemotherapy.[1] However, side effects and poor activity in certain types of cancer resulting from acquired or intrinsic resistance limit their clinical utility.[2,3] These limitations have stimulated the exploration of new metallodrugs with improved pharmacological properties, particularly with increased selectivity for cancer cells.

According to the original and empirical rules for the design of new bifunctional anticancer platinum(II) drugs, a *cis* geometry of leaving and nonleaving ligands (*i.e.* the complexes should contain two *cis* am(m)ine ligands and two *cis* anionic ligands) was a requirement for antitumor activity.[4,5] However, several new complexes of *trans* geometry have been identified that exhibit toxicity to tumor cell lines similarly to or even better than the analogous *cis* isomers and even cisplatin.[6,7] In addition, we demonstrated that simple encapsulation of an inactive platinum compound, transplatin (*trans* isomer of cisplatin), in phospholipid bilayers transforms it into an efficient cytotoxic agent[8] and that the toxicity of transplatin is markedly enhanced by UVA irradiation.[9] In particular, the latter observation was in agreement with other findings demonstrating that photoactivation or photopotentiation of platinum drugs can be one of the promising approaches to introduce novel platinum anticancer drugs with improved pharmacological properties.[10,11] Moreover, since the application of irradiation can be restricted exclusively to the tumor tissue, the resulting effects can be much more selective for the tumor.

Notably, the biological action of cisplatin is not significantly affected by irradiation with UVA or visible light.[9,12] On the other hand, the toxicity, in tumor cells, of the second generation cisplatin analogue carboplatin and its derivatives bearing 7-azaindole ligands can be markedly enhanced by UVA or visible light.[13,14] Other examples of antitumor photoactivatable platinum complexes are a triphenylamine-modified platinum–diimine complex which can be activated by red light[15,16] and platinum(IV) prodrugs containing azide ligands which can be activated by UVA or visible light.[11,17,18]

Despite the fact that there are several examples of photoactivatable platinum antitumor drugs, gaining an in depth understanding of the mechanisms by which these platinum complexes exert their photoactivated cytotoxic effects requires additional studies. Interestingly, mechanistic studies so far performed suggest that a common feature of photoactivation of platinum antitumor drugs is that their photoactivation results in altered DNA binding mode and damage. This might be of particular interest since binding to DNA represents a major step in the mechanism of action of antitumor platinum drugs.[19]

Very recently, we investigated the effect of a new bifunctional and mononuclear Pt(II) compound, *trans*-[$PtCl_2(NH_3)(L)$] (L = 1-methyl-7-azaindole, compound **1**, Fig. 1), on the growth and viability of human carcinoma cells as well as their putative mechanism(s) of cytotoxicity.[20] The results showed that substitution of 1-methyl-7-azaindole for ammine in ineffective transplatin resulted in a remarkable increase of the cytotoxic efficiency. The differences in the cytotoxic activities of **1** and transplatin were attributed to their different DNA binding modes. The presence of a 7-azaindole ligand in **1** also suggested that, similarly to carboplatin derivatives containing 7-azaindole ligands, also for **1** the cytotoxicity could be increased by irradiation with UVA or visible light.[14] Therefore, in the present work we investigated the photocytotoxic potential and molecular and cellular pharmacology of compound **1** under UVA radiation conditions. The results indicate that UVA light markedly potentiates the cytotoxicity of **1** and that the underlying mechanism involves ROS generation and DNA cleavage.

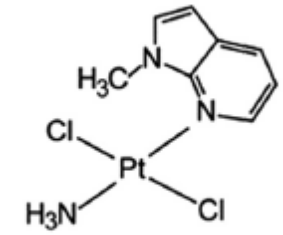

trans-[$PtCl_2(NH_3)(1M7AI)$]

Fig. 1 Structure of *trans*-[$PtCl_2(NH_3)(1M7AI)$] (compound **1**) used in this work; 1M7AI = 1-methyl-7-azaindole.

Experimental

Materials

Cisplatin, dimethyl sulfoxide (DMSO), ethidium bromide (EtBr), low gelling temperature agarose, neutral red, *N,N′*-dimethylformamide (DMF), ethylenediaminetetraacetic acid (EDTA), sodium chloride, HEPES [*N*-(2-hydroxyethyl)piperazine-*N′*-(2-ethanesulfonic acid)], sodium pyruvate, sodium hydroxide, 2,2,6,6-tetramethyl-4-piperidone (TMPD), Earle's Balanced Salt Solution (EBSS) and Triton X-100 were from Sigma-Aldrich (Prague, Czech Republic). Camptothecin was purchased from TopoGEN, Inc. (Florida, USA). 1-Methyl7-azaindole was from Ark Pharm, Inc. (Libertyville, USA). Compound **1** was prepared and characterized as already described.[20] It exhibits an absorption maximum at 294 nm and the absorption tail extends up to about 500 nm (ESI Fig. S2†). Stock solutions of **1** and cisplatin

were prepared at a concentration of 5×10^{-2} M in DMF, stored at 4 °C in the dark, and diluted with water to an appropriate concentration just before use. The final concentration of DMF was always kept at less than 0.1%. Stock solutions of platinum complexes for the cytotoxicity studies were also prepared in DMF and used immediately after preparation. The concentrations of platinum in the stock solutions were determined by flameless atomic absorption spectroscopy (FAAS). Plasmid pSP73KB (2455 bp) was isolated according to standard procedures. Calf thymus (CT) DNA (42% G + C, mean molecular mass ca. 20000 kDa) was prepared as previously described.[21,22] MTT [3-(4,5-dimethylthiazol-2-yl)-2,5-diphenyltetrazolium bromide] was from Calbiochem (Darmstadt, Germany). RPMI 1640 medium, fetal bovine serum (FBS), trypsin/EDTA, agarose and tris(hydroxymethyl) aminomethane (TRIS) were from PAA (Pasching, Austria). Penicillin and streptomycin were from Serva (Heidelberg, Germany).

Irradiation

DNA samples in a cell-free medium and cells were irradiated using an LZC-4V illuminator (photoreactor) (Luzchem, Canada) with a temperature controller and UVA (4.3 mW cm^{-2}; λ_{max} = 365 nm) tubes.

Effect of UVA irradiation on DNA modification by 1 in a cell-free medium

Closed circular pSP73 plasmid DNA (40 μg mL^{-1}) was mixed with the Pt complex in $NaClO_4$ (10 mM) or NaCl (10 mM) so that the r_i value was 0.02. The samples were then irradiated (UVA, λ_{max} = 365 nm) for the indicated time interval. After the irradiation was completed, samples were subjected to electrophoresis on 1% agarose gels running at 4 °C with a Trisacetate-EDTA (TAE) buffer and the voltage set at 20 V for 16 h (overnight). The gels were then stained with EtBr, followed by photography with a transilluminator. The intensity of fluorescence associated with bands was quantitated with the AIDA image analyzer software (Raytest, Germany).

Quantification of DNA binding in a cell-free medium

CT DNA (64 μg mL^{-1} or 2×10^{-4} M in phosphorus content) was mixed with **1** in $NaClO_4$ (10 mM) and immediately irradiated with UVA light at 37 °C or, for comparative purposes, kept at 37 °C in the dark. The molar ratio of the free platinum complex to nucleotide phosphates at the onset of incubation with DNA (r_i) was 0.1. Aliquots were removed at the indicated time intervals and quickly filtered using a Sephadex G-50 column to remove free (unbound) Pt. The Pt content in these DNA samples was determined by FAAS.

EPR spin-trapping spectroscopy

Electron paramagnetic resonance (EPR) spin-trapping spectroscopy was used to monitor the formation of $^1O_2$ (singlet oxygen) after UVA irradiation of pSP73 plasmid treated with **1**. Singlet oxygen was detected using the hydrophilic spin trapping compound TMPD.[23] To eliminate EPR signals due to impurities, TMPD was purified twice by vacuum distillation. Plasmid pSP73 was treated with **1** and incubated at 37 °C in the dark overnight. The r_b value was 0.02 (r_b is defined as the number of molecules of the platinum complex coordinated per nucleotide residue). Subsequently, plasmid DNA was kept in the dark for an additional 30 min or irradiated with UVA for 30 min in the presence of 50 mM TMPD. After the incubation/ irradiation period, samples of pSP73 previously treated with **1** were put in a glass capillary tube (Blaubrand®intraMARK, Brand, Germany) and EPR spectra were recorded using an EPR spectrometer, MiniScope MS300 (Magnettech GmbH, Berlin, Germany). EPR conditions were as follows: microwave power, 10 mW; modulation amplitude, 1 G; modulation frequency, 100 kHz; sweep width, 100 G; scan rate, 1.62 G s^{-1}; gain 500. Simulation of EPR spectra was done using Microsoft Excel 2010.

Cell lines and culture

The human ovarian carcinoma A2780 (parent cisplatin-sensitive) and human prostate adenocarcinoma LNCaP cell lines were supplied by Professor B. Keppler, University of Vienna (Austria). The A2780 cells were grown in RPMI 1640 medium supplemented with streptomycin (100 μg mL^{-1}), penicillin

(100 U mL^{-1}) and heat inactivated FBS (10%). The LNCaP cells were grown in PRMI 1640 medium supplemented with 10 mM HEPES, 1 mM sodium pyruvate, streptomycin (100 μg mL^{-1}), penicillin (100 U mL^{-1}) and heat inactivated FBS (10%). The cells were cultured in a humidified incubator at 37 °C under an atmosphere of 5% CO_2 and subcultured 2–3 times per week with an appropriate plating density.

Phototoxicity testing

Cells were seeded on 96-well tissue culture plates at a density of 10^4 cells per well in 100 μL of growth medium and left to adhere at 37 °C under a humidified 5% CO_2 atmosphere overnight. After washing cells with PBS, **1** was added into EBSS and incubated for 1 h under cultivation conditions. The final concentrations of **1** were in the range of 0 to 100 μM in a volume of 100 μL per well. The final DMF concentration in all wells was 0.1%, which was shown not to affect cell growth. After this time, cells were irradiated with UVA (λ_{max} = 365 nm) for 30 min. Following irradiation, EBSS with compound **1** was removed, the cells thoroughly washed with PBS, and then returned to the incubator in complete growth RPMI medium. Nonirradiated controls were tested as well. The phototoxicity was determined 24 h after irradiation using standard MTT assay. Briefly, 10 μL of MTT solution (5 mg mL^{-1}) was added to each well, and plates were incubated for 4 h. At the end of the incubation time the medium was removed and the formazan product was dissolved in 100 μL of DMSO per well. Cell viability was evaluated by measuring the absorbance at 570 nm (reference wavelength at 630 nm) using an Absorbance Reader Sunrise Tecan Schoeller. IC_{50} values (the concentration of the compound at which the compound caused death of 50% of the cells) were calculated from curves constructed by plotting cell survival (%) *versus* drug concentration (μM). All experiments were performed in triplicate. The reading values were converted to percentage of the control (% cell survival). Cytotoxic effects were expressed as IC_{50}.

Analysis of DNA fragmentation by single cell gel electrophoresis

DNA damage was studied by applying the comet assay (single cell gel electrophoresis), which is now the method of choice for measuring different kinds of DNA damage in cells.[24] The protocol used for the assessment of DNA damage in A2780 and LNCaP cells was in accordance with previously published work[25] with some modifications. Microscope slides were firstly precoated with 1% HMP (high melting point) agarose in phosphate buffered saline (PBS) and then placed in a drying oven at a temperature of 60 °C for at least 30 min. HMP agarose (1%, 100 μL) in PBS was applied on the precoated slides. The slides were then placed in a refrigerator in order to enhance gelling of the agarose. The human ovarian carcinoma A2780 and human prostate adenocarcinoma LNCaP cells were treated with the Pt complex at the final concentration of 10 μM for 1 h. For comparative purposes, cells treated with camptothecin (10 μM), which is a known DNA damaging agent, were tested as well (without irradiation). Samples were then irradiated with UVA (λ_{max} = 365 nm) for 30 min. Immediately after irradiation cells were collected by trypsinization and centrifuged (5 min, 2500 rpm) and cell pellets were dispersed in 20 μL of ice cold PBS. LMP (low melting point) agarose (1%, 80 μL) was added into this solution. The cell suspension was cast on the microscope slide to obtain a density of about 10000 nuclei per slide, covered by a glass cover slip to form a thin layer and moved to the refrigerator. After solidification, the cover slips were removed and the microscope slides were immersed in a lysis buffer [NaCl (2.5 M), EDTA (100 mM), Tris (10 mM), Triton X-100 (1%), pH = 10] at 4 °C for 24 h. After the lysis the slides were washed with distilled water to remove all salts, placed in an electrophoretic tank and dipped in a cool electrophoresis solution [NaOH (300 mM) and EDTA (1 mM)] for 40 min. Samples were then subjected to electrophoresis at 4 °C and 0.8 V cm^{-1} for 40 min. After the electrophoresis the slides were rinsed 3 times for 5 min with neutralisation buffer [Tris·HCl (0.4 M, pH = 7.5)]. The samples were subsequently stained with EtBr (ex. λ_{max} = 285 nm, em. λ_{max} = 605 nm). One hundred nuclei at randomly chosen visual fields from each sample were visually scored using an IX81 motorized inverted research microscope, CellR (Olympus), equipped with a DSU (Disk Scanning Unit) and a digital monochrome CCD camera, CCD-ORCA/ER. To avoid filter crosstalk, fluorescence was detected using HQ 545/30 exciter and HQ 610/75 emitter filter cubes (AHF Analysen Technique). The nuclei were divided, according to the intensity of DNA fragmentation, into five groups. The total damage to DNA in each sample was then determined as (0·N0) + (1·N1) + (2·N2) + (3·N3) + (4·N4), where 0–4 are the groups of damage intensity (group 4 = maximal damage) and N0–4 represent the number of cell nuclei present in the selected group.

Results and discussion

Effect of UVA irradiation on DNA modification by 1

The effect of UVA irradiation (λ_{max} = 365 nm) on DNA modification by **1** was assayed by agarose gel electrophoresis as described in the Experimental section. Careful inspection of the gels (Fig. 2) revealed that, when irradiated, **1** significantly affected the migration of both forms of plasmid DNA. The photoactivity induced by UVA light was reproducible and is intriguing, but there is a precedent for the activation of metal complexes with light at wavelengths where absorption is very low.[26–28] The reasons for this are currently not understood and require further investigation.

As shown in Fig. 2 (lanes 4–7), the mobility of the supercoiled (SC) form of plasmid DNA was gradually reduced with growing time of irradiation.

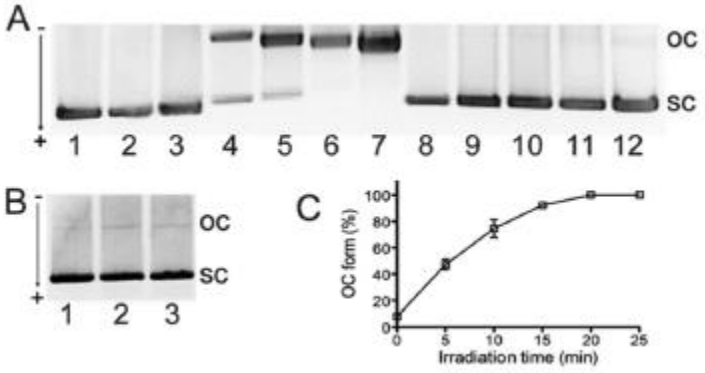

Fig. 2 Photoactivated reaction of **1** with pSP73 plasmid DNA in $NaClO_4$ (10 mM): panel A, lanes: **1**, control – nonirradiated DNA; 2, DNA irradiated for 25 min; lanes 3–7, DNA treated with **1** and irradiated for 0, 5, 10, 15 and 25 min, respectively; lanes 8–12, DNA treated with transplatin and irradiated for 0, 5, 10, 15 and 25 min, respectively. Panel B, lanes: 1, control, DNA kept in the dark for 30 min; lanes 2 and 3, DNA incubated for 30 min in the dark with 1 or transplatin, respectively. OC = open circle DNA; SC = super coiled DNA. Panel C, quantitative evaluation of photocleavage activity of **1** on irradiation with UVA. Symbols (mean ± SD, *n* = 3) represent percentage of nicked DNA in the reaction mixtures at the indicated time intervals.

This effect can result from increasing coordinative binding of **1** to plasmid DNA, reducing the negative superhelical density of DNA due to the unwinding of the double helix.[29] The irradiation of DNA in the presence of **1** also accelerated the mobility of the relaxed (open circular, OC) form. This effect can be interpreted to mean that with growing time of irradiation, the increasing binding of **1** to DNA also led to increasing the number of bifunctional adducts, which are known to shorten and condense the DNA helix.[30,31] Moreover, the most striking feature of these results (Fig. 2) was that the intensities of the bands corresponding to the relaxed (OC) form of DNA markedly increased during irradiation along with the concomitant decrease of the intensities of the supercoiled (SC) form. The irradiation of DNA in the presence of **1** for 15 min already led to the conversion of almost all molecules of SC DNA into an open-circular form (Fig. 2, lane 6). However, this effect was not observed for the samples irradiated in the absence of **1** (Fig. 2A, lane 2) or the samples incubated for 30 min with **1** in the dark (Fig. 2B, lane 2). This observation can be attributed to the formation of single strand breaks (ssb) in the DNA backbone, implicating DNA cleavage activity of **1** under irradiation.

For comparative purposes, identical experiments were also performed with transplatin. Under the same conditions as those used for the experiments with 1, there were no significant changes in the migration of pSP73 DNA incubated with transplatin for 0–25 min under irradiation conditions or in the dark (Fig. 2A, lanes 8–12 and 2B, and lane 3). As the only difference between the structures of **1** and transplatin consists in the replacement of one NH_3 group in transplatin with the 1M7AI ligand, the effects of UVA irradiation on the modifications of DNA interaction products with **1** appear to be dependent on the presence of the azaindole ligand.

To test whether the 1M7AI ligand itself is able to bind and/or cleave DNA, the same experiment as that performed with **1** (Fig. 2) was also performed with free 1M7AI. The results (ESI

Fig. S2†) clearly showed that free 1M7AI did not interact with plasmid DNA either in the dark or under UVA irradiation conditions.

In order to evaluate the effect of the composition of the incubation medium, an experiment described in ESI Fig. S2† was also performed in which DNA was incubated with **1** in the presence of NaCl (10 mM) and irradiated with UVA. The replacement of perchlorate by chloride in the incubation medium should suppress the hydrolysis of **1**, which is the rate-limiting step for DNA binding.[32] Interestingly, even at a relatively high concentration of chloride (4000 times higher than that of the platinum complex), results similar to those observed in $NaClO_4$ were obtained, *i.e.* even in NaCl (10 mM), **1** was able to change the DNA electrophoretic migration as well as to cleave plasmid DNA upon UVA irradiation (ESI Fig. S3†).

DNA binding kinetics

The data from the electrophoretic experiment (*vide supra*) were interpreted to mean that UVA light significantly facilitated DNA binding of **1** affecting the mobility of DNA through the agarose gel. To confirm this hypothesis, the kinetics of DNA binding of **1** to CT DNA was assessed by FAAS. DNA was mixed with **1** in $NaClO_4$ (10 mM) or NaCl (10 mM) and the sample was immediately irradiated with UVA light at 37 °C or kept at 37 °C in the dark. Aliquots were removed at the indicated time intervals and quickly filtered using a Sephadex G-50 column to remove free (unbound) Pt. The Pt content in these DNA samples was determined by FAAS.

As indicated in Fig. 3, UVA irradiation markedly potentiated the DNA binding ability of **1** in both $NaClO_4$ and NaCl compared to the situation in the dark. While there was a very low amount of platinum bound to DNA after 1 h of incubation in the dark (~2%), UVA irradiation of the mixture resulted in very fast binding so that complete binding of the platinum complex to DNA was observed in 1 h. Notably, there was almost no difference in the rate of DNA binding in the presence of ClO_4^- or Cl^- .

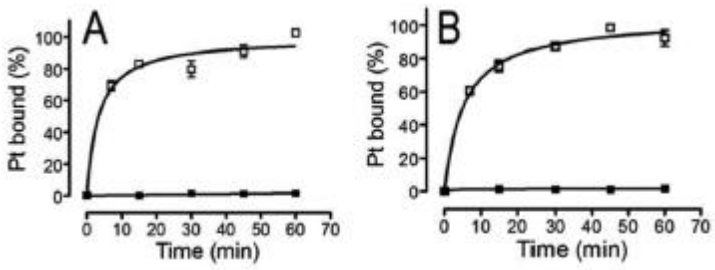

Fig. 3 Kinetics of binding of **1** to CT DNA in the dark (full symbols) or under UVA irradiation (open symbols). The reaction was performed in $NaClO_4$ (10 mM) (panel A) or NaCl (10 mM) (panel B). Symbols represent the mean ± SD from two independent experiments.

Formation of bifunctional DNA cross-links

The significant increase in electrophoretic mobility of the relaxed form of plasmid DNA incubated with **1** under irradiation conditions (Fig. 2) might be a consequence of the rise in bifunctional cross-links in the population of DNA adducts formed by **1**, which shorten and condense the DNA helix.[30,31] Therefore, a kinetic study of the conversion of the monofunctional adducts of **1** (formed in the first step of its binding to DNA) to bifunctional adducts under irradiation conditions or in the dark has been performed. CT DNA was incubated with **1** for 14 h in the dark at r_i value of 0.1. After this period, unbound molecules of **1** were removed and the sample was further incubated under UVA irradiation conditions or in the dark at 37 °C for additional 30 min. Aliquots were withdrawn at the indicated time intervals and treated with thiourea to remove monofunctionally bound platinum. After exhaustive dialysis, the amount of platinum remaining bound to DNA was measured by FAAS. As indicated in Fig. 4, after 14 h of incubation in the dark, ~42% of total platinum bound to DNA was contained in bifunctional cross-links. Under UVA irradiation, the fraction of bifunctional adducts quickly grew so that after 20 min of irradiation, almost all platinum was bound bifunctionally. In contrast,

the monofunctional adducts of **1** evolved to bifunctional cross-links much more slowly in the dark so that no significant increase in the percentage of bifunctional adducts was detectable after 30 min.

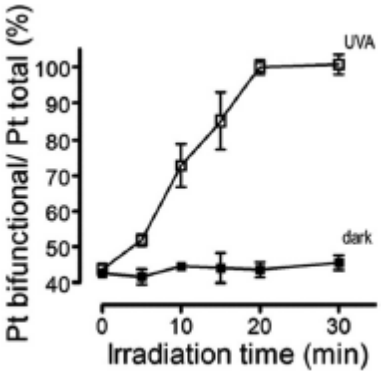

Fig. 4 Kinetics of closure of monofunctional adducts into bifunctional cross-links in the dark (full symbols) or under irradiation (open symbols). Symbols represent the mean ± SD from two independent experiments, each performed in triplicate.

A significant accrual in the amount of bifunctional adducts was only detectable for much longer periods of incubation in the dark. After 24 h of incubation in the dark, ~18% of monofunctional adducts were transformed into bifunctional cross-links so that the number of bifunctional adducts increased from 42 to 60% in this time interval. This result suggests that UVA light effectively facilitated the closure of monoadducts formed in DNA by **1** into bifunctional cross-links.

A prerequisite of the formation of bifunctional DNA adducts in DNA by bidentate platinum(II) complexes, such as cisplatin, transplatin and their derivatives, is their propensity to lose both chloride ligands. The lack of ability of transplatin to readily form bifunctional cross-links is believed to be the reason for its lack of anticancer activity.[33,34] It has been shown[9] that UVA light promotes the loss of the second chloride of transplatin. Thus, it is reasonable to suggest that UVA light also promotes the loss of the second chloride of **1** thereby facilitating the formation of bifunctional cross-links by this agent under irradiation conditions.

DNA photocleavage mechanism

As indicated above, 1, when irradiated with UVA, was able to effectively cleave DNA backbone. To elucidate the mechanism of the DNA cleavage, the photocleavage of pSP73 plasmid DNA in the presence of **1** and of different inhibitors was investigated (Fig. 5). Since DNA cleavage was not inhibited in the presence of hydroxyl radical (OH•) scavengers such as mannitol and DMSO (Fig. 5A, lanes 3 and 4, respectively), the hydroxyl radical is unlikely to be responsible for cleavage. In the presence of superoxide dismutase (SOD), an effective quencher of the superoxide anion radical (O_2^-), cleavage was slightly but significantly enhanced (Fig. 5A, lane 5). This effect can be partly attributed to increased production of singlet oxygen ($^1O_2$) and an electron-transfer process.[35] To test the possibility that photoinduced cleavage involves formation of singlet oxygen, the cleavage experiment was carried out in the presence of sodium azide, one of the most effective singlet oxygen quenchers.[36] As indicated in Fig. 5A (lane 6), cleavage of pSP73 was significantly inhibited in the presence of sodium azide. This suggests that production of $^1O_2$ is likely to be responsible for the DNA cleavage reaction.

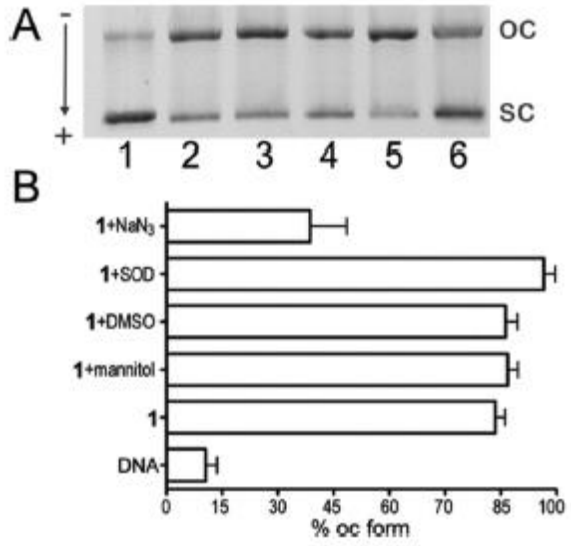

Fig. 5 (A) Photoactivated cleavage of pSP73 in the presence of 1 (r_i= 0.02) and different inhibitors after irradiation with UVA light for 10 min in Tris·HCl (10 mM, pH 7.4). Lane 1: pSP73 in the absence of 1 and no inhibitor; lane 2: pSP73 and 1, no inhibitor; lane 3: in the presence of mannitol (100 mM); lane 4: in the presence of DMSO (200 mM); lane 5: in the presence of superoxide dismutase (1000 U ml^{-1}); lane 6: in the presence of sodium azide (10 mM). (B) Bar-graph representation of the effect of inhibitors on the UVA-activated cleavage activity of **1**.

EPR spin-trapping spectroscopy

To further support the role of $^1O_2$ in the photocleavage activity of **1**, the EPR spin-trapping technique was used. The spin-trapping was accomplished by utilizing the oxidation of hydrophilic diamagnetic TMPD by $^1O_2$ known to yield paramagnetic 2,2,6,6-tetramethyl-4-piperidone-1-oxyl (TEMPONE).[23,37] The TEMPONE EPR spectra of plasmid DNA treated with 1 were recorded immediately after irradiation of the samples with UVA light for 15 or 30 min. Nonirradiated controls were tested as well. In the samples treated with 1 and irradiated for 15 or 30 min, significant TEMPONE EPR signals were observed (Fig. 6).

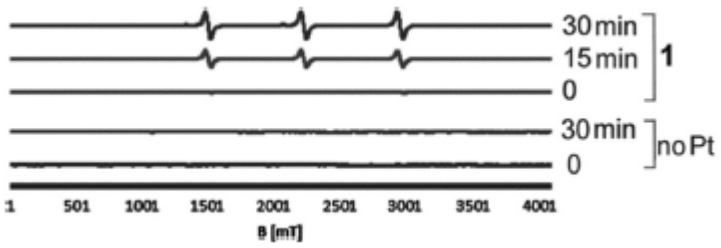

Fig. 6 Detection of singlet oxygen by EPR spin-trapping spectroscopy. EPR spectra werere corded for solutions of pSP73 DNA either untreated or treated with **1** and nonirradiated or irradiated with UVA for 15 and 30 min.

The addition of TMPD to control pSP73 plasmid DNA incubated with **1** under continuous irradiation for 30 min did not result in the appearance of TEMPONE EPR signals. Therefore the $^1O_2$ production during the irradiation period was a consequence of photoactivation of the platinum compound. This result is consistent with DNA cleavage following the production of singlet oxygen.

DNA cleavage in living cells

The results described above demonstrated that irradiation of **1** in the presence of DNA resulted in cleavage of the DNA sugar– phosphate backbone and induction of single-strand breaks (ssb). Therefore, the next experiment was intended to determine whether this process can take place also in living cells. For this purpose, we first determined whether **1** can enter the cell nucleus and bind to DNA. The degree of DNA platination was determined by inductively coupled plasma mass spectrometry (ICP-MS) for the human ovarian carcinoma cell line A2780 after its exposure to **1**, cisplatin, or transplatin (2 or 20 μM) for 5 or 24 h (Table S1†). After both 5 and 24 h exposure times, DNA platination was comparable for 1 and cisplatin. Notably, for transplatin DNA platination was markedly lower. Overall, DNA platination appears to be consistent with the view and supports the hypothesis that, similarly to cisplatin, **1** can effectively enter the nucleus of tumor cells and platinate DNA. Hence, this result suggests that DNA is a likely biological target also for **1**.

To demonstrate that irradiation of **1** in the presence of DNA can result in cleavage of the DNA sugar-phosphate backbone and induction of ssb can take place also in living cells, single cell gel electrophoresis experiments (comet assays) were performed. The values of total DNA damage obtained in A2780 and LNCaP cells treated with **1** and irradiated with UVA for 30 min are plotted in Fig. 7. Camptothecin, which is known to induce ssb by trapping covalently linked topoisomerase–DNA cleavage complexes,[38] was used as a positive control.

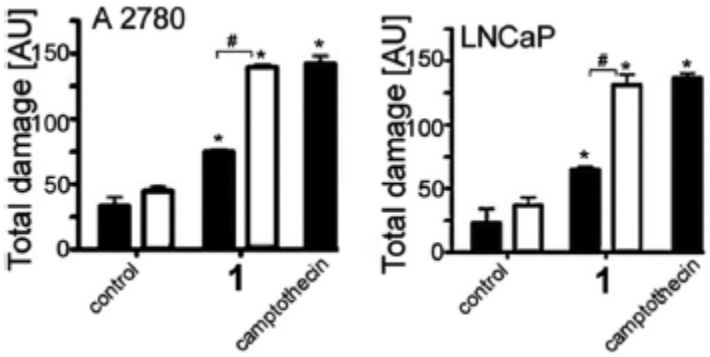

Fig. 7 Effect of **1** when UVA irradiated (30 min) or in the dark (white or black bars, respectively) on DNA damage in A2780 and LNCaP cells investigated by the comet assay. Camptothecin was included in the experiment as a positive control. The mean values and standard deviations obtained in three independent experiments are reported. The symbol (*) denotes a significant difference ($p < 0.01$) from the control; (#) denotes a significant difference ($p < 0.01$) between the effects of **1** UVA irradiated and in the dark.

In this assay the production of DNA-strand breaks results in migration of DNA from the cell nucleus. Treatment of cells with **1** in the dark only resulted in a slight increase of migration of DNA from the cell nucleus, confirming that a small number of DNA strand breaks took place (Fig. 7, black bars). However, this extent of DNA strand cleavage was much lower than that caused by camptothecin. As **1** does not cleave DNA in the cell-free experiments performed in the dark, it is reasonable to assume that the damage observed in the cellular experiments performed in the dark was a consequence of other cellular processes activated as a response to the cell damage caused by treatment with **1** (for instance, excision DNA repair, programmed cell death etc.). In contrast, irradiation with UVA significantly increased DNA migration from cells treated with **1** (Fig. 7, white bars), which is consistent with the presence of an increased amount of DNA strand breaks. Importantly, the ability of **1** to cause DNA damage in human cancer cells increased markedly after irradiation for both A2780 and LNCaP cell lines.

Photocytotoxicity

DNA strand breaks are considered to be toxic lesions, a major threat to genetic stability and cell survival. Thus, the findings described above prompted us to test whether UVA light may influence the cytotoxic activity of **1** in human cancer cells. As is described in detail in the Experimental section, the tumor cells A2780 were treated with **1** for 1 h (the final concentrations of **1** were in the range of 0 to 100 μM). After this time, cells were irradiated with UVA (λ_{max} = 365 nm) for 30 min. The

phototoxicity was determined 24 h after irradiation. The photoinduced inhibition of cell viability by **1** in human ovarian carcinoma cells A2780 is summarized in Fig. 8. Upon irradiation, the survival rate of A2780 cells markedly decreases with the increasing concentration of **1** in contrast to the survival rate of nonirradiated A2780 cells which changed very little with the increasing concentration of **1**. The corresponding IC_{50} values were (32.26 ± 0.37) μM and (1.42 ± 0.08) μM for A2780 cells treated with **1** in the dark or under UVA irradiation, respectively. The results clearly showed that A2780 cells were approximately 22-fold more sensitive to **1** when irradiated compared to the treatment in the dark. Thus, the results are consistent with the thesis that UVA irradiation markedly potentiates **1** in killing human cancer cells.

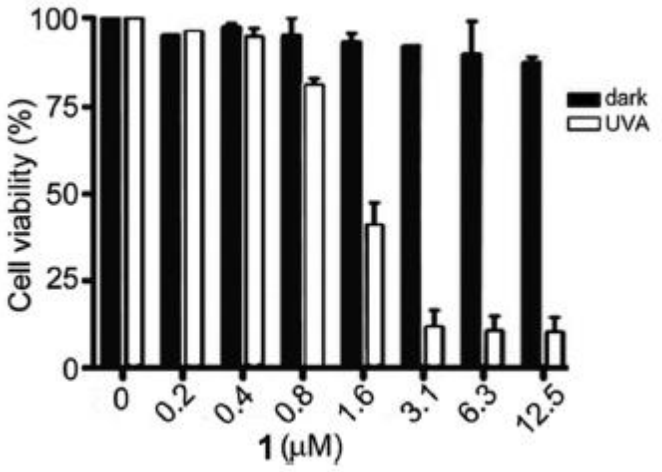

Fig. 8 The viability of A2780 cells incubated with different concentrations of **1** for 1 h when irradiated or sham irradiated (for 30 min). The concentration of **1** was in the range of 0–12.5 μM. The phototoxicity was determined 24 h after irradiation.

Conclusions

The present work describes photoinduced DNA damage by a derivative of ineffective transplatin, *trans*-[$PtCl_2(NH_3)$(1-methyl7-azaindole)] (**1**), and the photocytotoxic activity of this compound. The DNA binding rate of **1** in a cell-free medium is markedly accelerated by UVA light. Notably, the enhanced DNA binding is attended by markedly elevated formation of the more toxic bifunctional cross-links compared to the situation in the dark. It is therefore reasonable to suggest that both the enhanced efficiency of formation and structural impact caused by the cross-links formed by UVA-irradiated **1** contribute to the markedly enhanced cytotoxicity of irradiated **1** in comparison with nonirradiated **1**.
It has been also shown that **1**, due to the presence of the 1-methyl-7-azaindole ligand, can generate reactive singlet oxygen and that its production is responsible for ssb in DNA also in living cells treated with irradiated **1**. Hence, DNA damage (cleavage) resulting from the generation of singlet oxygen has been proposed to significantly contribute to the potentiated cytotoxic activity of **1** under UVA light as well. The effects described in this study suggest that compound **1** or its derivatives might be potential candidates for photodynamic therapy. Despite the fact that this compound shows some anticancer activity even in the dark, the considerable increase in activity under irradiation conditions may allow to administer much lower doses than those needed for conventional therapy (without irradiation). This implies that many of the limiting side effects of conventional chemotherapy by metallodrugs could be avoided because only the tumor tissue would be locally irradiated. Hence, the compound in tumor cells would be activated to kill preferentially these cells. Clearly discernible, emerging current trends in the design of new anticancer metallodrugs are the departure from the cisplatin paradigm of activity. Thus, the discoveries described in this report open the door to a new large family of photoactivatable metal-based drug candidates.

Acknowledgements

This work was supported by the Czech Science Foundation (grant 14-21053S), the National Program of Sustainability I (LO1204), a student project of Palacký University (IGAPrF 2016 013), and the University of Bari and the Consorzio Interuniversitario di Ricerca in Chimica dei Metalli nei Sistemi Biologici (C.I.R.C.M.S.B.). We acknowledge that our participation in the EU COST Action CM1105 enabled us to exchange regularly the most recent ideas in the field of metallodrugs with several European colleagues.

Notes and references

1 N. J. Wheate, S. Walker, G. E. Craig and R. Oun, Dalton *Trans*., 2010, 39, 8113–8127.
2 V. Brabec and J. Kasparkova, Drug Resist. Updates, 2005, 8, 131–146.
3 L. Kelland, Nat. Rev. Cancer, 2007, 7, 573–584.
4 B. Rosenberg, J. Clin. Hematol. Oncol., 1977, 7, 817–827.
5 M. J. Cleare, P. C. Hydes, B. W. Malerbi and D. M. Watkins, Biochimie, 1978, 60, 835–850.
6 M. Coluccia and G. Natile, Anti-Cancer Agents Med. Chem., 2007, 7, 111–123.
7 S. M. Aris and N. P. Farrell, Eur. J. Inorg. Chem., 2009, 1293– 1302.
8 O. Vrana, V. Novohradsky, Z. Medrikova, J. Burdikova, O. Stuchlikova, J. Kasparkova and V. Brabec, Chem. – Eur. J., 2016, 22, 2728–2735.
9 P. Heringova, J. Woods, F. S. Mackay, J. Kasparkova, P. J. Sadler and V. Brabec, J. Med. Chem., 2006, 49, 7792– 7798.
10 F. S. Mackay, J. A. Woods, P. Heringova, J. Kasparkova, A. M. Pizarro, S. A. Moggach, S. Parsons, V. Brabec and P. J. Sadler, Proc. Natl. Acad. Sci. U. S. A., 2007, 104, 20743– 20748.
11 P. J. Bednarski, F. S. Mackay and P. Sadler, Anti-Cancer Agents Med. Chem., 2007, 7,75–93.
12 J. Kasparkova, H. Kostrhunova, O. Novakova, R. Křikavová, J. Vančo, Z. Trávníček and V. Brabec, Angew. Chem., Int. Ed., 2015, 54, 14478–14482.
13 J. Mlcouskova, J. Stepankova and V. Brabec, J. Biol. Inorg. Chem., 2012, 17, 891–898.
14 P. Štarha, Z. Trávníček, Z. Dvořák, T. Radošová-Muchová, J. Prachařová, J. Vančo and J. Kašpárková, PLoS One, 2015, 10, e0123595.
15 Z. Zhang and X. Dong, BioMetals, 2009, 22, 283–288.
16 Z. Zhang, R. Dai, J. Ma, S. Wang, X. Wei and H. Wang, J. Inorg. Biochem., 2015, 143,64–68.
17 A. M. Pizarro, R. J. McQuitty, F. S. Mackay, Y. Zhao, J. A. Woods and P. J. Sadler, ChemMedChem, 2014, 9, 1169– 1175.
18 G. Ragazzon, I. Bratsos, E. Alessio, L. Salassa, A. Habtemariam, R. J. McQuitty, G. J. Clarkson and P. J. Sadler, Inorg. Chim. Acta, 2012, 393, 230–238.
19 T. C. Johnstone, K. Suntharalingam and S. J. Lippard, Philos. *Trans*. R. Soc., A, 2015, 373, 20140185.
20 J. Pracharova, T. Saltarella, T. Radosova Muchova, S. Scintilla, V. Novohradsky, O. Novakova, F. P. Intini, C. Pacifico, G. Natile, P. Ilik, V. Brabec and J. Kasparkova, J. Med. Chem., 2015, 58, 847–859.
21 V. Brabec and E. Palecek, Biophys. Chem., 1976, 4, 79–92.
22 V. Brabec and E. Palecek, Biophysik, 1970, 6, 290–300.
23 J. Moan and E. Wold, Nature, 1979, 279, 450–451.
24 J. M. Enciso, O. Sánchez, A. López de Cerain and A. Azqueta, Mutagenesis, 2015, 30,21–28.
25 C. Ersson and L. Möller, Mutagenesis, 2011, 26, 689–695.
26 D. Loganathan and H. Morrison, Photochem. Photobiol., 2006, 82, 237–247.
27 N. J. Farrer, J. A. Woods, V. P. Munk, F. S. Mackay and P. J. Sadler, Chem. Res. Toxicol., 2009, 23, 413–421.
28 V. Brabec, J. Pracharova, J. Stepankova, P. J. Sadler and J. Kasparkova, J. Inorg. Biochem., 2016, 160, 149–155.
29 M. V. Keck and S. J. Lippard, J. Am. Chem. Soc., 1992, 114, 3386–3390.
30 G. L. Cohen, W. R. Bauer, J. K. Barton and S. J. Lippard, Science, 1979, 203, 1014–1016.
31 W. M. Scovell and F. Collart, Nucleic Acids Res., 1985, 13, 2881–2895.
32 E. R. Jamieson and S. J. Lippard, Chem. Rev., 1999, 99, 2467–2498.
33 M. Boudvillain, R. Dalbies, C. Aussourd and M. Leng, Nucleic Acids Res., 1995, 23, 2381–2388.
34 M. Leng, A. Schwartz and M. J. Giraud-Panis, in Platinum-Based Drugs in Cancer Therapy, eds. L. R. Kelland and N. P. Farrell, Humana Press Inc, Totowa/NJ, 2000, pp. 63–85.
35 N. M. Shavaleev, H. Adams, J. Best, R. Edge, S. Navaratnam and J. A. Weinstein, Inorg. Chem., 2006, 45, 9410– 9415.

36 J. R. Kanofsky, Photochem. Photobiol., 1991, 53,93–99.
37 S. Wei, J. Zhou, D. Huang, X. Wang, B. Zhang and J. K. Shen, Dyes Pigm., 2006, 71,61–67.
38 Y. Pommier, Nat. Rev. Cancer, 2006, 6, 789–802.